JCRS

Journal of Chemical Reactivity and Synthesis 2023: 13(4) 266-285

Research Article

First Principles calculation High Spin to Low Spin transition in the $SrMnO_3$ and the $CaMnO_3$ compound

Narges Saki, Azadeh Aezami

Departments of Physics, Ahvaz Branch, Islamic Azad University, Ahvaz, Iran

ARTICLE INFO:

Received:
11 November 2023

Accepted:
21 December 2023

Available online:
24 December 2023

✉: A. Aezami
a.aezami@gmail.com

ABSTRACT

In this research, structural, electronic, magnetic, and electrical properties of $SrMnO_3$ and $CaMnO_3$ have been investigated using calculations based on density-functional theory from scratch and Quantum-Espresso calculation code. The Hubbard parameter has been calculated for the Mn atom using a linear response approach and LDA+U approximation for both compounds. This parameter is 3.5 eV for $CaMnO_3$ and it is 3.1 eV for $SrMnO_3$. The calculations showed that even though both compounds are insulator and G-type antiferromagnetic materials. Results reveal that both materials are in stable HS and LS states in pressures higher and lower than -10 GPa and -20 GPa, respectively. Moreover, the magnetic moment of $CaMnO_3$ in the pressure of -20.51 GPa decreases from $3.41\mu_B$ in a stable HS state to 1.44 μ_B in an LS state, and that of $SrMnO_3$ in the pressure of -26.87 GPa declines from 4.37 μ_B in HS state to 1.55 μ_B in LS state.

Keywords: Density Functional Theory, High Spin, Low Spin, enthalpy, $SrMnO_3$, $CaMnO_3$

1. Introduction

Recent developments in the First Principle approach to investigate the ideal perovskite with a general formula $AMnO_3$ are examined because they present remarkable ferroelectricity [1],

piezoelectric [2], and ferromagnetism [3] properties. Significant research has been carried out on perovskite materials and manganese. $CaMnO_3$ assumes an orthogonal structure but is also considered a cubical perovskite archetype [4, 5], deformed by the rotation or angulation of a normal MnO_6 octagon by an octagonal MnO_6 process. $CaMnO_3$ is a frequency associated with the $SrMnO_3$ compound since it displays a similar behavior [6, 7].

Given that $SrMnO_3$ perovskite is polymorphous with a complex magnetic order and polarization, it is a multi-ferric material and has attracted a great deal of attention [8-12]. Based on the average size of the Sr^{2+} ion, cubic and hexagon polymorphisms are indicated for $SrMnO_3$ [13]. When the temperature exceeds 1035°C, the hexagon structure changes to a high-temperature cube [14]. The high-temperature cubic $SrMnO_3$ may be quenched and preserved as an unstable compound at low temperatures [15]. Recent studies have shown that $SrMnO_3$ is stable in orthogonal, hexagonal, and cubic structures at various temperatures. Specifically, the cubic structure of $SrMnO_3$, with its high symmetry, has aroused great fondness for its rich magnetic properties and potential applications [10-12, 16, 17].

Nevertheless, magnetic and rich behaviors have been reported in cubic $SrMnO_3$ with doping or deformation approaches [12, 15, 18, 19], whereas the ground-state is still oppositely theoretically. It has been reported experimentally that the G-type antiferromagnetic sequencing can be transferred to the C-type antiferromagnetic sequencing in cubic $SrMnO_3$ by doping Ce or La [12]. The cubic structure of $SrMnO_3$ with G-type antiferromagnetic and paraelectric arrangements is stable by epitaxial strains [11] and leads to an interesting ferroelectric-ferromagnetic state. Consequently, the epitaxial strains and doping vectors in the cubic structure of $SrMnO_3$ become the driving force for the magnetic phase transfer between the different antiferromagnetic phases and even between the phases of antiferromagnetic and ferromagnetic. The phase transfer due to pressure is iso structural.

Theoretically, density functional theory has been widely used to clarify the pressure-induced phase transition in transition metals oxide [20-22].

This paper investigates the behavior of cubic structures $SrMnO_3$ and $CaMnO_3$ by first-principles calculations using the LDA+U approximation. The different parts of this manuscript are as follows. In section II, we examine the computational and Structural method used in this article. Section III presents the results and discussion: subsection IIIA describes the results of the magnetic and electronic properties of cubic $SrMnO_3$ and $CaMnO_3$, and subsection IIIB describes the effect of pressure on the magnetic and electrical properties of cubic $SrMnO_3$ and $CaMnO_3$. The final section includes the conclusion.

2. Computational and Structural method

Many materials' electronic and magnetic properties are accursed within the density functional theory (DFT) [23]. This manuscript uses the plane wave method and open-source Quantum-Espresso code [24] to perform the calculations. The pseudo potentials are generated using ultra soft conditions and conducted using the local density approximation+ Hubbard (LDA+U). Since the Mn atom has a 3d orbital, the LDA+U method is used to describe better the electronic structure of $SrMnO_3$ and $CaMnO_3$. We have calculated Hubbard U with linear response approach [25-30] using the wave pseudo potential method implemented in Quantum-Espresso code for Mn in the $SrMnO_3$ and $CaMnO_3$, respectively, and it is in accordance with other reported calculations. A linear response approach is proposed that in internally consistent with the chosen definition for the occupation matrix of the relevant localized orbitals. We have calculated Hubbard U on the Mn atoms with moderate value of 3.1 eV and 3.5 eV for $SrMnO_3$ and $CaMnO_3$, respectively [31-34].

Theoretical lattice constants obtained in our calculations were 3.823 $\mathring{A}$ and 3.810 $\mathring{A}$ for the $SrMnO_3$ and $CaMnO_3$, respectively, which our results are in good agreement with experimented results [16, 35]. We have used an energy cutoff 50 Ry and 60 Ry for the plane

wave expansion for $SrMnO_3$ and $CaMnO_3$, respectively, and a 6×6×6 grid for both compounds. The accuracy of the total energy calculations was 10^{-10} Ry are used for the cubic structures. We have schematically shown the crystalline structures of $SrMnO_3$ and $CaMnO_3$ in Fig. 1. Structural optimization has been performed for the pressure range. Possibility of different magnetic state high spin or low spin is explored by performing the structural optimization with different initial magnetization. For lower spin, convergence was achievable only for high spin while low spin state become metastable for $CaMnO_3$ and $SrMnO_3$ P ~ -20.51GPa and P ~ -26.87 GPa, respectively. Calculations are also performed without any symmetry constrains. However, the optimized structures obtained from such calculations were similar to the one found for cubic symmetry. This suggests that cubic phase is stable throughout the pressure range presented in this work. The atomic simulation technique employed in the present study is based on energy minimization procedures, at 0K without considering any thermal motion in the material. The details of the simulation mythology are explained elsewhere [15,24].

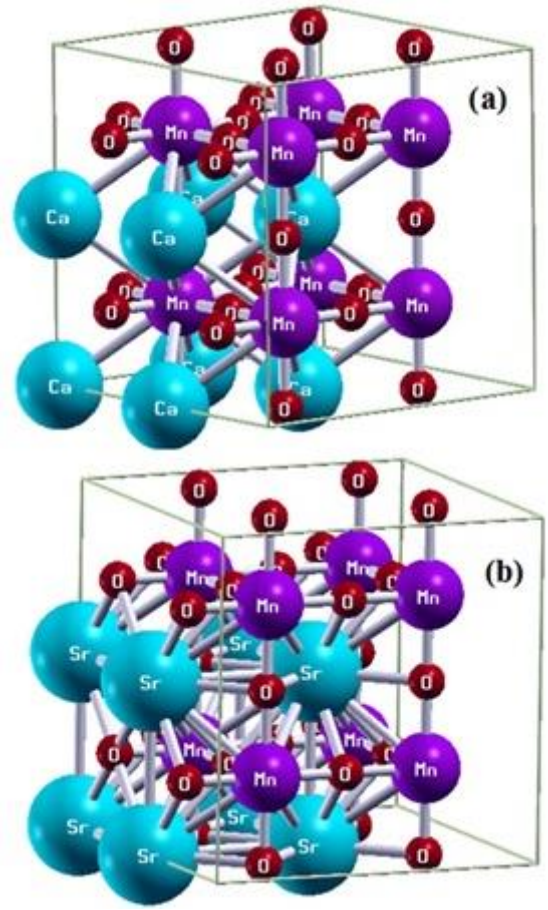

Fig. 1. The crystal structure of perovskite oxide CaMnO3 (a) and SrMnO3 (b).

3. Result and discussion

3.1 Discuss the magnetic and electronic properties

In this study, after investigating the structural, electronic, magnetic, and electrical properties of two $SrMnO_3$ and $CaMnO_3$ compounds with LDA+U approximation without applying pressure, structural properties, crystal energy, band gap, and magnetic moment in each four ferromagnetic, A, C, and G-type antiferromagnetic orderings were optimized (If the spin orientation of the atoms is in the direction of the xy-plane of ferromagnetic, but in the direction of the z-axis of antiferromagnetic is A-type antiferromagnetic , If the spin orientation of the atoms is in the direction of the xy-plane of the antiferromagnetic but in the direction of the z axis of the ferromagnetic is C-type antiferromagnetic, If the spin orientation of the atoms is in the direction of the xy-plane and in the direction of the z-axis of the

antiferromagnetic is G-type antiferromagnetic). The calculations show that both compounds have the most stable state in the G-type antiferromagnetic sequence. The essential and effective parameter U (screened Coulomb energy) was calculated using a linear response approach to consider the coherence property between electrons. Hubbard parameter of $CaMnO_3$ was 3.5 eV, and that of $SrMnO_3$ was 3.1 eV.

B_0 Represents the bulk modulus and B' is the pressure derivative of the bulk modulus. The estimation obtained from this equation gives B_0= 148.90 GPa and 158.15 GPa for $SrMnO_3$ and $CaMnO_3$, respectively. This is in good agreement with the theoretical value observed. The theoretical value of B_0 and B' for both modifications are given in Table1.

Table1. Shows the difference in the results of calculations related to $SrMnO_3$ and $CaMnO_3$ with G-type antiferromagnetic configuration compared with experimental and theoretical results.

	$CaMnO_3$(G-AFM)			$SrMnO_3$(G-AFM)		
	Our calculation	Exp	Other Calculation	Our calculation	Exp	Other calculation
Space group	Pm3m[37]			Pm3m [36]		
Lattice parameter	3.810 $(\mathring{A})$	3.805 $(\mathring{A})$ [35]	3.745 $(\mathring{A})$ [37]	3.823 $(\mathring{A})$	3.804 $(\mathring{A})$ [39]	3.824 $(\mathring{A})$ [40]
Mn (μ_B)	2.68	2.65[36]	2.44[38]	2.82	2.60 ± 0.2[16]	2.47[40]
B_0	158.15(GPa)		252[37]	148.90(GPa)		166[41]
B'	5.10		7.8[36]	3.98		4.70[41]
$K(GPa)^{-1}$	0.0063			0.0067		
E_{gap}	0.25(eV)		0.22[38]	0.0075		0.22[42]

From structural studies, it can be seen that the large bulk modulus corresponding to both $CaMnO_3$ and $SrMnO_3$ compounds being more prominent than 1000 GPa is an indicator of

their low compressibility and high rigidity. The derivative of bulk modulus concerning pressure is of paramount physical importance indicating the dependency of bulk modulus on pressure. Applying bulk modulus and its derivative with respect to time, crystal volume can be calculated when exposed to external pressure.

The calculated spin moment, as is seen in Table 1, for G-type antiferromagnetic ordering for Mn atom in $CaMnO_3$ and $SrMnO_3$ are 2.68 μ_B and 2.82 μ_B, with the error of %0.03 and %0.08 to experimental values being 2.65 μ_B [36] and 2.60 μ_B, respectively. The results from a total and partial density of states of $CaMnO_3$ under the influence of the Hubbard parameter (LDA+U approximation) show that G-type antiferromagnetic ordering is the stable magnetic ordering for this compound.

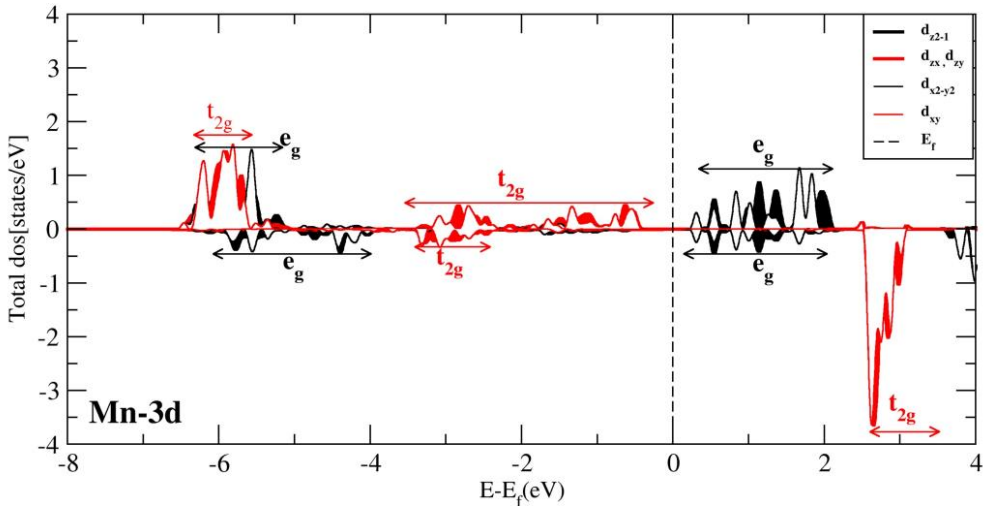

Fig.2. show the spin-projected total density of states for Mn-3d $CaMnO_3$, the ground state G-AFM state is found to be an insulator with a band gap of approximately 0.25 eV.

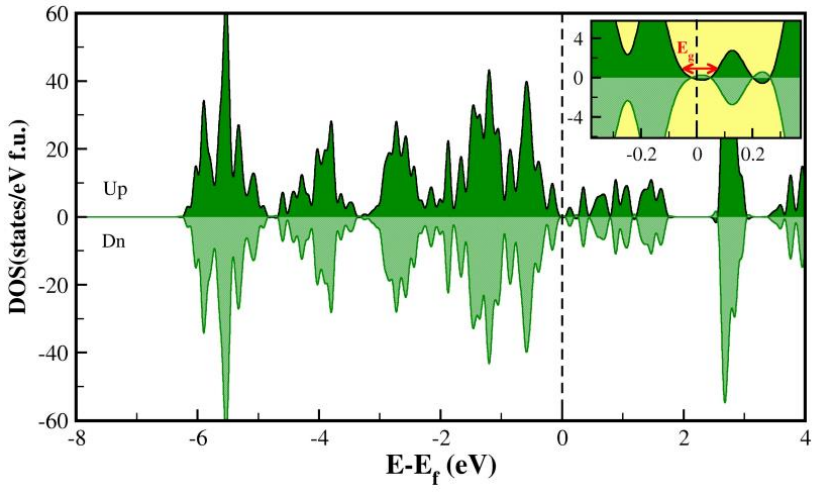

Fig.3. show the total density of states for $CaMnO_3$, the ground state G-AFM state is found to be an insulator.

To investigate the contribution of atomic orbitals to the $CaMnO_3$ compound, the partial density of state of 3d, 4s, and 2p orbitals of respectively Mn, Ca, and O atoms were calculated, ranging from -8 to 4 eV. Considering that 3d and 2p orbitals of sequentially Mn and O are near to be filled, the contribution of these orbitals is more, and as they have enormous contribution near the Fermi level, a band gap is formed between these states. The overlap between these orbitals at the end of the valence band and conduction band, above the Fermi level, shows that electrons of these orbitals are the origin of the bond formation between atoms. This overlap indicates the presence of a covalent bond between Mn and O atoms. The results suggest that the electrons of the Mn atom are not completely localized near the Fermi level. Taking it into account that the electrons of Mn, because of large occupation in orbitals, are the main reason for the magnetic properties of this compound, the partial density of states, and the range of, e_g and t_{2g} orbitals of Mn atom in $CaMnO_3$ have been calculated. As shown in Fig. 2, the electrons of the e_g level are located broadly in the conduction band near the Fermi level. In majority and minority spin states, $d_{x^2-y^2}$ and d_{3z^2-1} orbitals are dominant orbitals, and electrons of t_{2g} level are localized in farther regions from the Fermi level. The study of the results related to the spin phase of G-type ferromagnetic ordering shows that the partial density of state corresponding to the majority and minority

spins in Mn atoms are symmetric. Therefore, these atoms show a magnetic property in the mentioned compound.

Furthermore, surveying the calculated electronic density of the state of the Mn atom demonstrates that at the Fermi level, the density of states related to this atom is more than those of other atoms. Thus, it can be revealed that the electrons' contribution to this atom is more in the appearance of some $CaMnO_3$ physical properties, including electrical conductivity and magnetic property. According to the partial density of the state of $CaMnO_3$, it is realized that for all spin orderings in the majority and minority spin states, 3d and 2p orbitals of respectively Mn and O atoms have the most contribution to the valence band. But, the conduction band 3d orbital of Mn plays an important role which stems from the way of contribution of different orbitals of an atom to the formation of its density of state. The orbitals near the Fermi level are of more significance due to their role in forming the bond between atoms, band gap, and probable transition between conduction and valence band. It is crucial to notice that the sum of the partial density of states never equals the total density of states, for spheres around the atoms, do not occupy the whole space around the unit cell. Another noticeable impact shown in the partial density of state calculated for Mn atoms for ferromagnetic and antiferromagnetic phases is that the partial density of states of Mn atoms in the antiferromagnetic state is narrower (have less broadening) with respect to the ferromagnetic state. In order to investigate the reason of such property, 3d orbital of Mn atom has to be studied more carefully. Taking into account that the electrons of Mn atom are not localized near Fermi level, while the orbital of t_{2g} level is localized. It is observed in Fig. 2 that the electrons of e_g level lie widely near Fermi level in conduction band that $d_{x^2-y^2}$ and d_{3z^2-1} orbitals are predominant in majority and minority spin states, respectively. The maximum stability occurs when axial orbitals of e_g level located along the z axis have been more stable and lie lower to $d_{x^2-y^2}$ axial orbitals. In other words, the system is more stable in

the z-axis direction. As electrons always tend to lie at a more stable level, the electrons of e_g level lie in $d_{3z}{}^{2}{}_{-1}$ orbital. G-type antiferromagnetic phase has been analyzed (Fig. 3).

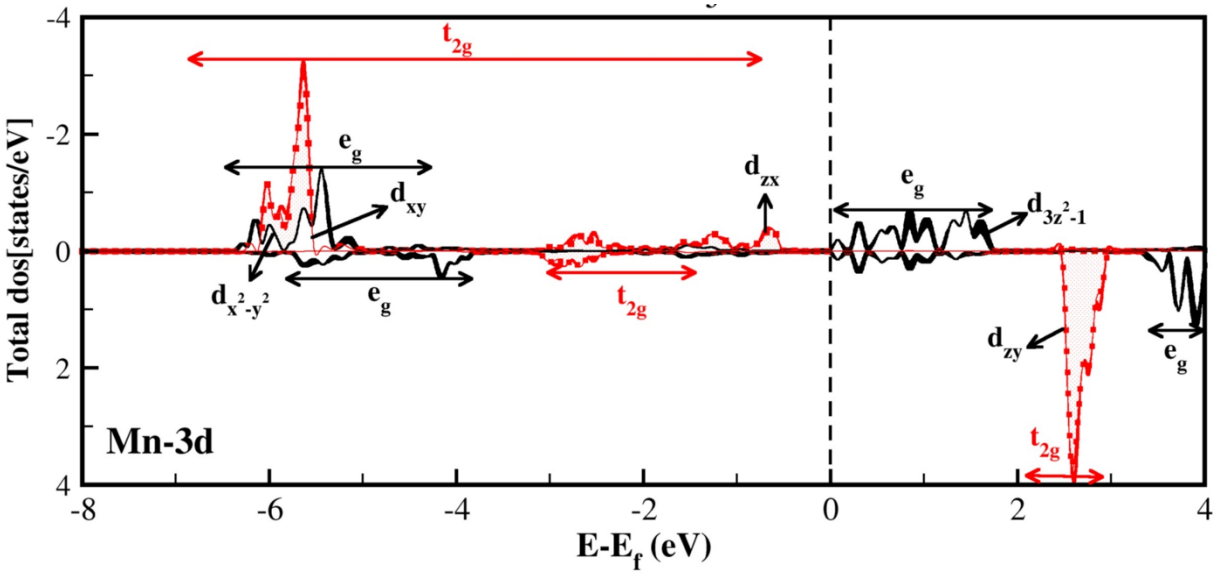

Fig.4. show the spin-projected total density of states for Mn-3d $SrMnO_3$, the ground state G-AFM state is found to be an insulator.

Fig. 4 shows Pdos for 3d-orbitals of Mn atom in the cubic $SrMnO_3$ with G-type antiferromagnetic configuration from LDA+U with U=3.5 eV. The Fermi level is set with vertical dotted lines at zero energy. We will discuss the $SrMnO_3$ oxide cubic structure on this ground state in the following. Due to the negligible contribution of Sr atoms in the partial density of states of the mentioned compounds, it can be concluded that a strong ionic bond has been established between Sr and the crystal lattice. Near the valence band, the major contribution of the density of state is the 3d orbital of the Mn atom and the 2p orbital of the O atoms. It can also be seen that in the conduction band, the most significant effect is often from the 3d orbital of the Mn atom. In addition, even if the Mn atom is in the ground state of the antiferromagnetic octagonal structure, it does not have three pairs of spins in the crystal field. In each Mn atom, there are many minority-spin states in the valence band. There are states at the Fermi level that are mainly 3d-Mn orbitals. The 2p-O orbital also contributes significantly due to its hybridization with 5s-Sr, 3d-Mn, and 4s-Mn orbitals, but the 3p-Mn

orbital is near the Fermi level and has minimal contributions. Strong hybridization in the valence band can be observed between the 3d-Mn and 2p-O orbitals. At the bottom of the valence band, the strong hybridization is mainly from the 3d orbital of the Mn atom.

Due to their crystalline effects, the octagonal structure of the Mn atoms in the $SrMnO_3$ cubic compound produces two- and three-fold degenerate orbitals, $t_{2g,}$ and e_g 3d-Mn orbitals (see Fig. 4). In Mn oxide, the ligand field division is smaller than the exchange division, and the mixed e_g/t_{2g} properties are observed in the valence and conduction band. It can be seen in Fig. 4 that the upper of the valence band is mainly Mn $3d_{3z}{}^2{}_{-1}$. Mn $3d_{yz}$ and Mn $3d_{xz}$ have the same property due to the xy symmetry of the unit cell. Mn $3d_{3z}{}^2{}_{-1}$ behaves very differently from other e_g orbitals due to the significant deformation of the structure along the z-axis in the unit cell, which is the source of the deformation effect in the opening of the large $SrMnO_3$ band gap. With the Hubbard parameter (U) introduction, the Fermi level has a gap, and insulating property of $SrMnO_3$ is shown [15].

The calculation of partial and total density of states of $CaMnO_3$ and $SrMnO_3$ compounds under the influence of the Hubbard parameter for G-type antiferromagnetic configuration shows that both compounds have insulator-like properties electrically, which is in line with the experimental findings [35-43].

3.2 Discuss pressures effects on cubic $SrMnO_3$ and $CaMnO_3$

In this part, both compounds are exposed to %5 to %20 pressure in positive pressure (compressive Pressure (CP)) and negative Pressure (Tensile Pressure (TP)). To investigate two compounds in different pressures, considering the thermodynamic dE=-PdV equation and the equality between the derivative of the Murnaghan equation and -PdV gives equation 1:

$$V(P)=V_0\left[\left(\frac{B'}{B_0}P\right)+1\right]^{-1/B'} \qquad (1)$$

Where P is the external pressure applied to the system.

The changes in energy gap and other properties of $SrMnO_3$ compound for positive and negative pressures have been shown in Fig. 5, bearing in mind that the ground state is G-type antiferromagnetic, and this spin ordering has insulator like behavior. According to this figure, by the increase in pressure in a positive direction, the width and intensity of the peaks have changed, and the compound has remained an electrical insulator. The energy gap has changed with applying pressure in a negative direction and increasing by a few percentages. The Fermi level intersects the density of states in both spin channels, and the compounds change into a metallic phase. According to energies obtained, it is concluded that the system becomes unstable by increasing pressure in both positive and negative directions. Applying pressure shows more overlap of wave functions in this situation, and electronic repel leads to a repulsive potential and energy bands shifts. It is observed that by pressure increase due to more overlap of wave functions, hybridization of bonds has increased, and the curve of the density of states is broadened.

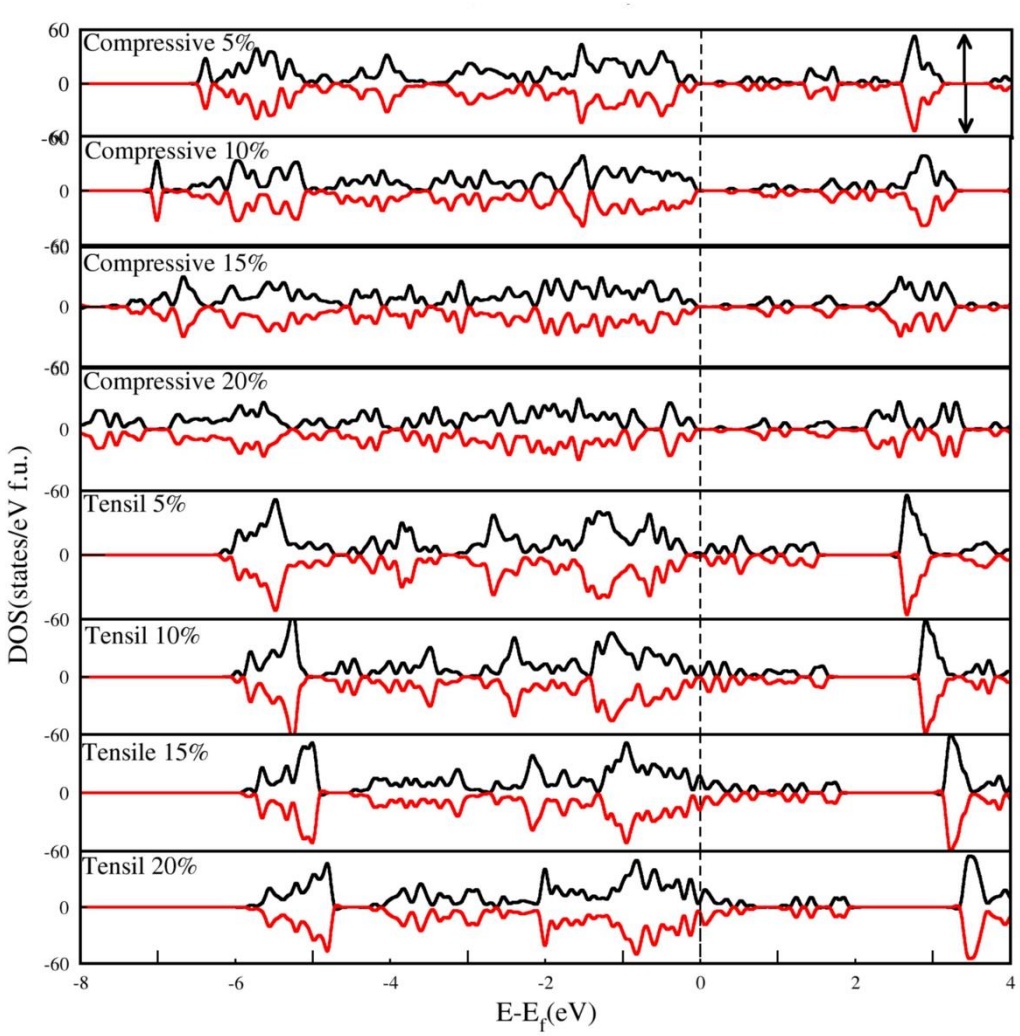

Fig.5. show the total density of states for $SrMnO_3$, under the influence of tensile and compressive pressure from 5% to 20%. The vertical dashed line shows the location of Fermi energy.

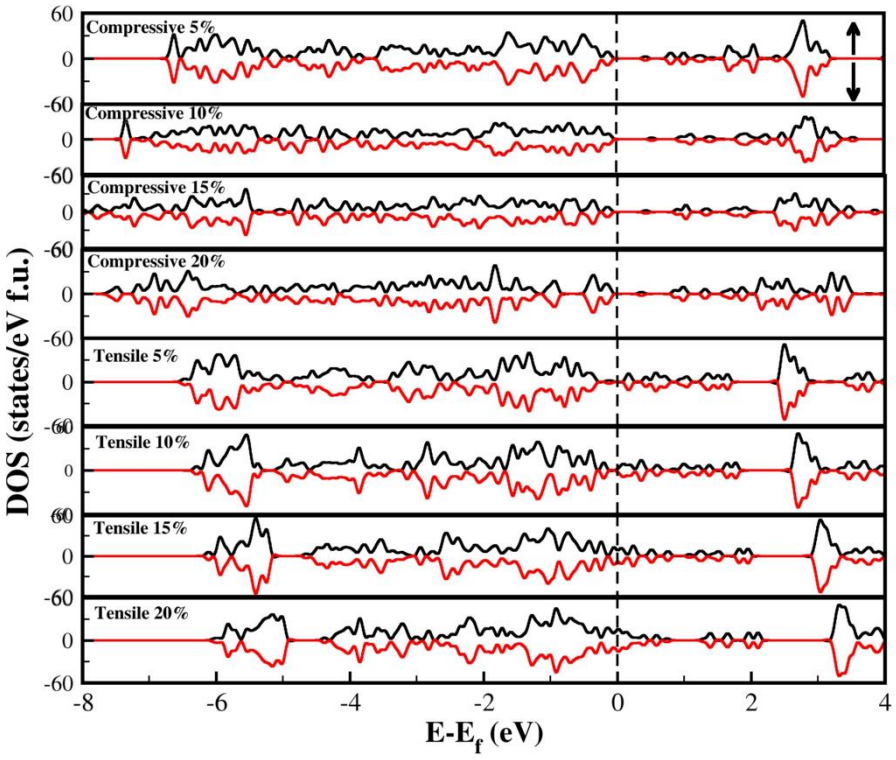

Fig.6. total density of states for $CaMnO_3$, under the influence of tensile and compressive pressure from 5% to 20%. The vertical dashed line shows the location of Fermi energy.

The calculations for the $CaMnO_3$ compound also show that this compound in the ground state has a G-type antiferromagnetic cubic structure and is an electrical insulator with a band gap of 0.25 eV. As the results of the calculations of applying compressive and tensile pressure have been shown in Fig. 6, with the increase in pressure in a positive direction (compressive), just the intensity and width of peaks have changed. Still, electrical-wise, the compound has yet to remain an insulator. However, applying pressure in a negative direction and increasing it by %10 has changed the band gap. Fermi level has intersected density of states in both spin channels, and the compound behaves like a metal. The calculation results reveal that by pressure increase due to more overlap of wave functions, hybridization of bonds has increased, and as a result, the curve of density states is broadened in this state. The energy calculations of $SrMnO_3$ and $CaMnO_3$ compounds for G-type antiferromagnetic spin ordering in TP (Tensile Pressure) and CP (Compressive Pressure) have been listed in Table 2.

Table2. difference in the total energy of $CaMnO_3$ and $SrMnO_3$ in tensile and compressive pressures from 5% to 20%.

pressure	Total energy of $CaMnO_3$ (eV)		Total energy of $SrMnO_3$ (eV)	
Compressive (5%)	-514.93625498	Insulator	-515.45326589	Insulator
Compressive (10%)	-514.21016981	Insulator	-515.25654589	Insulator
Compressive (15%)	-513.78297058	Insulator	-514.51236548	Insulator
Compressive (20%)	-513.64883366	Insulator	-513.45326589	Insulator
Tensile (5%)	-514.02249909	Insulator	-514.42120741	Insulator
Tensile (10%)	-513.99449060	Metal	-514.39583671	Insulator
Tensile (15%)	-513.95918399	Metal	-514.36458935	Metal
Tensile (20%)	-513.92351022	Metal	-514.33253331	Metal

Corresponding to the calculation results shown in Fig. 5 and Fig. 6 as well as Table 2, the optimum energy of the $CaMnO_3$ compound obtained after applying pressure has increased by an increase in pressure in both positive and negative directions, and the system has become unstable. Due to the rise in pressure in the positive direction, the results show that the bond length of Mn-O has decreased from 1.8853 Å to 1.5082Å, and a repulsive potential is formed. By increasing pressure in the opposite direction, the bond has formed a length increase to 2.2624 Å. The similar calculation results for the $SrMnO_3$ compound also show that an increase in pressure in the positive direction has decreased the bond length of Mn-O from 1.9115 Å to 1.6821 Å, and an increase in pressure in the negative direction increased the bond length to 2.3703 Å.

The results of energy calculations in terms of volume, shown in Table3, indicate that through the slope calculation of the line connecting the points related to the G-type antiferromagnetic phase of $CaMnO_3$, the applied pressure is almost between -26 GPa and 148 GPa, and the same calculations reveal that it is from -23 GPa to 124 GPa. for $SrMnO_3$ compound. From calculation results of the change in volume as expected, the increase in volume, in both compressive and tensile pressure, results in respectively decrease and

increase in volume; however, this increase or decrease is not noticeable, and it is the confirmation of low compressibility and high rigidity of both $CaMnO_3$ and $SrMnO_3$ compounds and in accord with their bulk modulus results. On the other hand, gap energy in different pressure depends on parameters such as temperature, bulk modulus, a derivative of bulk modulus, and the like. In conclusion, the band gap of two compounds, under pressure, might increase or decrease under the influence of the pressure.

Table3. the difference in the tensile and compressive pressures from 5% to 20%.

	Pressure of $CaMnO_3$ (GPa)		pressure of $SrMnO_3$ (GPa)	
Compressive (5%)	38.81	Insulator	18.64	Insulator
Compressive (10%)	62.11	Insulator	50.35	Insulator
Compressive (15%)	117.42	Insulator	89.53	Insulator
Compressive (20%)	148.01	Insulator	124.04	Insulator
Tensile (5%)	-10.84	Insulator	-18.18	Insulator
Tensile (10%)	-17.34	Metal	-20.19	Insulator
Tensile (15%)	-18.26	Metal	-21.63	Metal
Tensile (20%)	-26.02	Metal	-23.29	Metal

To find the possible transition from high spin (HS) to low spin (LS), enthalpy has been calculated for the HS and LS modes. At lower pressures, convergence was possible only for the HS mode, while the LS mode showed instability for P>-10 GP, P>-20 GPa for $CaMnO_3$ and $SrMnO_3$, respectively. In Fig. 7 and Fig. 8, the enthalpy is shown as a function of pressure. Although the HS state is stable for P<-10 GPa,P<-20 GPa for $CaMnO_3$ and $SrMnO_3$, respectively. Also, LS and HS cross enthalpies at P~ -20.51 GPa and P~ -26.87 GPa for $CaMnO_3$ and $SrMnO_3$, respectively. The Mn magnetic moment as a function of pressure is shown in Figs. 7 and 8. According to the diagrams, it can be concluded that with increasing pressure, the magnetic moment decreases slowly. Fig. 7 shows a significant drop in the magnetic moment from 3.41 μ_B in HS mode to 1.44 μ_B in LS mode for $CaMnO_3$ at -20.51 GPa. Fig. 8 shows this significant drop for the $SrMnO_3$ compound at -26.87 GPa, and the

magnetic moment decreased from 4.37 μ_B in the HS mode to 1.55 μ_B in the LS mode. Therefore, the results obtained from enthalpy diagrams and magnetic moments show the transition from HS mode to LS mode at P~ -20.51 GPa and -26.87 GPa for $CaMnO_3$ and $SrMnO_3$, respectively.

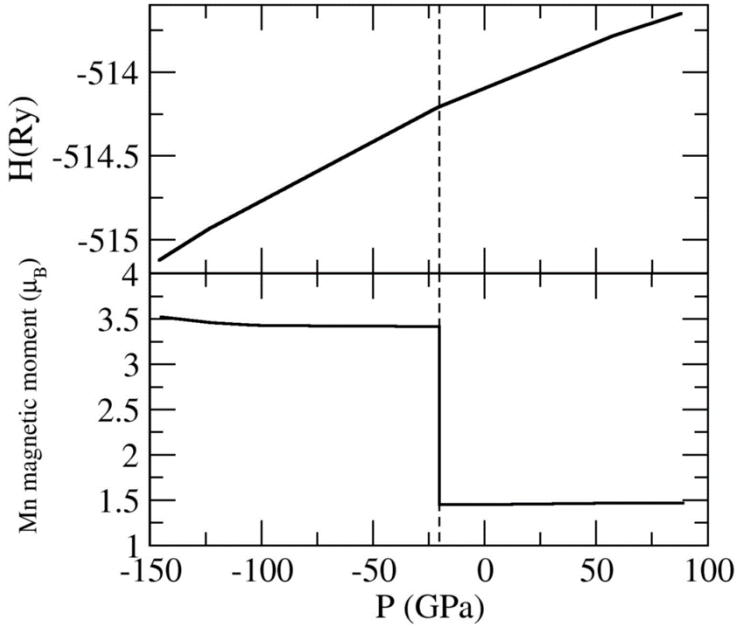

Fig.7. above plot show the Enthalpy (H) $CaMnO_3$ of HS and LS states as a function of pressure. Bottom plot shows the impact of pressure on Mn magnetic moment.

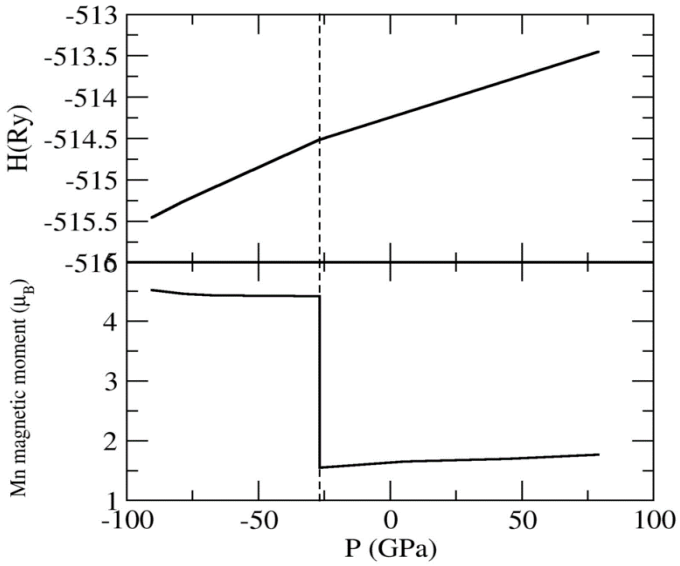

Fig.8. above plot show the Enthalpy (H) $SrMnO_3$ of HS and LS states as a function of pressure. Bottom plot shows the impact of pressure on Mn magnetic moment.

4. Conclusion

In summary, we investigated the structural, electronic, magnetic, and electrical properties of $SrMnO_3$ and $CaMnO_3$ using density-functional theory and Quantum-Espresso calculation code. The Huhard parameters for $CaMnO_3$ and $SrMnO_3$ respectively 3.5 eV and 3.1 eV have calculated. The results showed that the both compounds are insulator and G-type antiferromagnetic materials. Also, we have studied the effect of pressure on these compounds for %5 to %20 in tensile pressure (TP) and compressive pressure (CP) direction along the z-axis, after that the transition from HS to LS of both compounds has been investigation through the results of enthalpy calculations in terms of pressure. Results showed that both $SrMnO_3$ and $CaMnO_3$ are in stable Hs and LS states in pressures higher and lower than -10 Gpa and -20 Gpa sequentially. Furthermore, the $CaMnO_3$ in the pressure of -20.51 Gpa subtraction from 3.41μB in a stable HS state to 1.44 μB in the LS state magnetic moments, for $SrMnO_3$ in the pressure of -26.87 Gpa decreases form 4.37 μB in Hs state to 1.55 μB in LS states.

Acknowledgments

The current study was partially supported by the Ahvaz Branch of Islamic Azad University. The authors would like to thank the Research Council for their generous support of this work.

References

[1] J. G. Bednorz, K. A. Muller, Phys. Rev. Lett. 52 (1984) 2289-2292.

[2] S. F. Hichernell, IEE. 52 (2005) 737-745.

[3] S. Cabuk, H. Akkus, A. M. Mamedov, Phys. B. 394 (2007) 81-85.

[4] W. E. Pickett, D. J. Singh, Phys. Rev. B. 53 (1996) 1146-1160.

[5] M. Nicastro, C. H. Patterson, Phys. Rev. B. 65 (2002) 205111-205118.

[6] S. Keshavarz, Y. O. Kvashnin, D. C. M. Rodrigues, M. Pereiro, I. D. Marco, C. Autieri,

L. Ordstr¨om, I. V. Solovyev, B. Sanyal and O. Eriksson, Phys. Rev. B. 95 (2017)115120 - 115128.

[7] N. T. Trang, B. T. Cong, P. H. Thao, P. T. Tan, N. D. Tho, H. N. Nhat, Phys. B. 406 (2011) 3613–3621.

[8] X. Zhu, A. Edström, C. Ederer, Phys. Rev. B. 101 (2020) 064401-064409.

[9] A. Kumar, M. Kumar, R. P. Singh, P. K. Singh, Solid, State, Comm . 324 (2021) 114139 - 114148.

[10] Z. Fang, I. V. Solovyev, K. Terakura, Phys. Rev. Lett. 84 (2000)3169-3172.

[11] J. H. Lee, K. M. Rabe, Phys. Rev. Lett. 104 (2010) 207204-207209.

[12] H. Sakai, S. Ishiwata, D. Okuyama, A. Nakao, H. Nakao, Y. Murakami, Y. Taguchi, Y. Tokura, Phys. Rev. B. 82 (2010) 180409-1800412.

[13] Y. Syono, S. I. Akimoto, K. Kohn, J. Phys. Soc. Jpn. 26 (1969) 993-999.

[14] T. Negas, J. Solid, State, Chem. 7 (1973) 85-88.

[15] R. Søndena, P. Ravindran, S. Stølen, T. Grande, M. Hanfland, Phys. Rev. B. 74 (2006) 144102-144108.

[16] T. Takeda, S. Ohara, J. Phys. Soc. Jpn. 37 (1974) 275-275.

[17] A. Sacchetti, M. Baldini, P. Postorino, C. Martin, A. Maignan, J. Raman. Spec. 37 (2006) 591-596.

[18] M. Y. Kagan, D. I. Khomskii, M. V. Mostovoy, Eur. Phys. Journal. B. 12 (1999) 217-223.

[19] Y. Tokura, Reports on Progress in Physics. 69 (2006) 797-851.

[20] R. E. Cohen, I. I. Mazin, and D.G .Isaak, Science. 275 (1997) 654-657.

[21] J. Kunes, A. V. Lukoyanov, V. I. Anisimov, R. T. Scalettar, and W. E. Pikett, Nature. Mat. 7 (208) 198-202.

[22] G. Trimarchi and N. Binggeli, Phys. Rev. B. 71 (2005) 035101-035107.

[23] P. Hohenberg, W. Kohn, Phys. Rev. B. 64 (1964) 136-142.

[24] Quantum Espresso home page, http;//www.quantum-espresso.org.

[25] M. Cococcioni, et al., Phys. Rev. B. 71 (2005) 035105-035111.

[26] V. I. Anisimov, et al., J. Phys.: Condens. Matter. 9 (1997) 767-771.

[27] V. I. Anisimov, et al., Phys. Rev. B. 48 (1993) 16929-16934.

[28] I. V. Solovyev, et al., Phys. Rev. B. 50 (1994) 16861-16871.

[29] A. I. Liechtenstein, et al., Phys. Rev. B. 52 (1995) R5467-R5470.

[30] W. E. Pickett, et al., Phys. Rev. B. 58 (1998) 1201-1209.

[31] B. R. Nada, and S. Satpathy, Phys. Rev. Lett. 101 (2008) 127201-127206.

[32] E. Dagotto, T. Hotta, and A. Moreo, Phys. Reports. 344 (2001) 1-153.

[33] J. Kanamori, J. Appl. Phys. Ics. 31(1960) 45-235.

[34] K. Janicka, et al, J. Appl. Phys. 103 (2008) 07B508-07B512.

[35] A. S. Verma, V. K. Jindal, J. Alloys. Compounds. 485 (2009)514-518.

[36] E. O. Wollan, W. C. Koehler, Phys. Rev. 100 (2955) 545-563.

[37] N. Hamdad, B. Bouhafs, J. Phys. B. 405 (2010) 4595-4606.

[38] N. T. Trang, et al., J. Phys. B. 406 (2011) 3613-3621.

[39] A A Belik, et al., Phys. Rev. B. 84 (2011) 094438-094442.

[40] R. Sondena. S. Stolen. P. Ravindran, phys. Rev. B. 75 (2007) 184105-184110.

[41] R. Sondena, et al., Phys. Rev. B. 74 (2006) 144102-144109.

[42] C. L. Ma, et al., Phys. Lett. A. 374 (2010) 2388 -2391.

[43] Z. Zeng, M. Greenblatt, M. Croft, Phys. Rev. B. 59 (1999) 8784-8788.